

Frequency Response Analysis of a Single-Area Power System with a Modified LFC Model Considering Demand Response and Virtual Inertia

Authors:

Muhammad Saeed Uz Zaman, Syed Basit Ali Bukhari, Khalid Mousa Hazazi, Zunaib Maqsood Haider, Raza Haider, Chul-Hwan Kim

Date Submitted: 2020-06-23

Keywords: steady-state error, virtual synchronous generator, virtual inertia, demand response, system frequency response, load-frequency control

Abstract:

The modern electric power system is foreseen to have increased penetration of controllable loads under demand response programs and renewable energy resources coupled with energy storage systems which can provide virtual inertia. In this paper, the conventional model of an electric power system is appended by considering, individually and collaboratively, the role of demand response and virtual inertia for the purpose of frequency analysis and control. Most existing literature on this topic either considers one of these two roles or lacks in providing a general model of power system with demand response and virtual inertia. The proposed model is presented in general form and can include/exclude demand response and/or virtual inertia. Further, power system operator can opt the power shares from conventional, demand response, and virtual inertia loops for frequency regulation and can also evaluate the impact of other parameters such as time delays and frequency deadbands on system frequency response. The mathematical formulation of steady-state values of frequency deviation and power contribution from all resources is provided and validated by simulation results under various scenarios including a case of wind intermittency.

Record Type: Published Article

Submitted To: LAPSE (Living Archive for Process Systems Engineering)

Citation (overall record, always the latest version):

LAPSE:2020.0742

Citation (this specific file, latest version):

LAPSE:2020.0742-1

Citation (this specific file, this version):



LAPSE:2020.0742-1v1

DOI of Published Version: <https://doi.org/10.3390/en11040787>

License: Creative Commons Attribution 4.0 International (CC BY 4.0)

Article

Frequency Response Analysis of a Single-Area Power System with a Modified LFC Model Considering Demand Response and Virtual Inertia

Muhammad Saeed Uz Zaman , Syed Basit Ali Bukhari , Khalid Mousa Hazazi, Zunaib Maqsood Haider, Raza Haider and Chul-Hwan Kim *

College of Information and Communication Engineering, Sungkyunkwan University, Suwon 16419, Korea; saeed568@skku.edu (M.S.U.Z.); s.basit41@skku.edu (S.B.A.B.); khazazi@skku.edu (K.M.H.); zmhaider@skku.edu (Z.M.H.); razahaider@skku.edu (R.H.)

* Correspondence: chkim@skku.edu; Tel.: +82-31-290-7166

Received: 14 February 2018; Accepted: 26 March 2018; Published: 29 March 2018



Abstract: The modern electric power system is foreseen to have increased penetration of controllable loads under demand response programs and renewable energy resources coupled with energy storage systems which can provide virtual inertia. In this paper, the conventional model of an electric power system is appended by considering, individually and collaboratively, the role of demand response and virtual inertia for the purpose of frequency analysis and control. Most existing literature on this topic either considers one of these two roles or lacks in providing a general model of power system with demand response and virtual inertia. The proposed model is presented in general form and can include/exclude demand response and/or virtual inertia. Further, power system operator can opt the power shares from conventional, demand response, and virtual inertia loops for frequency regulation and can also evaluate the impact of other parameters such as time delays and frequency deadbands on system frequency response. The mathematical formulation of steady-state values of frequency deviation and power contribution from all resources is provided and validated by simulation results under various scenarios including a case of wind intermittency.

Keywords: load-frequency control; system frequency response; demand response; virtual inertia; virtual synchronous generator; steady-state error

1. Introduction

The frequency profile of an electric power system is among the fundamental indicators of the system's stability and security. The system frequency, which is dependent on real power balance, is required to be maintained within a specific operating range even though the power system continuously experiences fluctuations in power generation and demand. Therefore, frequency control is one of the primary control objectives in the design and operation of an electric power system. The aim of frequency control is to ensure power system's stable frequency profile by balancing power generation and demand while adhering to the requirements of system protection [1]. Traditionally, spinning and non-spinning reserves balance the power generation and demand to regulate the system frequency. However, it is not an environment-friendly and economic approach. The modern power system will have increased penetration of renewable energy systems (RES), generally coupled with energy storage systems (ESS), and a significant portion of curtailable loads [2]. These responsive loads and ESS have great potential to balance the grid power and have advantages over conventional methods. This work presents a modified model of a single-area electric power system for the purpose of frequency analysis and control by considering the effects of demand response and ESS.

According to the most accepted definition, demand response (DR) refers to the changes in the electricity usage by demand-side resources from their regular consumption patterns. DR programs are driven by the reasons of network resiliency and economy and, therefore, are broadly categorized into two categories: incentive-based (or dispatchable) programs and time-based (non-dispatchable) programs. In the modern smart grid era, DR offers multifarious services. It can be used to financially incentivize the utility companies and the customers [3–9], neutralize the impacts of intermittency of RES [10–13], provide ancillary services and mitigate the voltage and frequency fluctuations [14–21], and has several other diverse purposes such as transmission expansion planning [22] and improved transformer utilization [23].

Similar to DR, RES and ESS have increased importance in the modern power system. The high penetration of RES in modern power system is inevitable, but the benefits of integrating RES are accompanied by several challenges related to system protection and control (e.g., voltage rise due to bi-directional power flows, power fluctuations due to the intermittency of RES, and poor frequency regulation) [24–26]. In the conventional electric power system, most of the electrical power comes from synchronous machines and the contribution of distributed or RES is trifling. In the large synchronous machines, the inherent kinetic energy due to rotor inertia and damping effect due to mechanical friction and electrical losses in machine windings play a significant role in the grid stability. On the other hand, the power units derived by RES have either very small or no rotating mass resulting in degraded inertia and damping properties [1,27,28]. The negative impact of reduced inertia and damping properties on grid's dynamic performance is accelerated when penetration level of RES increases. A way to stabilize an RES-integrated grid is to deliver the inertia virtually. For this purpose, ESS-like batteries are utilized in coordination with power electronics-based converters and a control system. In this way, a significant share of RES in power grids can be realized without compromising system's reliable and stable operation. This concept is also known as virtual synchronous generator (VSG), used in this paper, and virtual synchronous machine (VISMA) [1,29,30]. There is a substantial rise in research work on this topic [31,32], and recent studies show the promising results of VSG in grid stability [33–37]. The contribution and highlights of this paper are summarized as follows:

1. The conventional model of an electric power system used for analysis and control of system frequency is modified to include separate control loops for the DR and the VSG controls. The provision of these control loops provides extra degrees of freedom for frequency regulation and a better system structure for controller design.
2. The proposed model provides the system operator with the opportunity to select the power share from DR, VSG, and/or conventional control for frequency regulation. The effects of time delays, frequency deadbands, and power shares are explained, individually as well as combined, for DR and VSG controls. Further, the impact of unregulated wind generation is also demonstrated and important conclusions have been drawn.
3. This work contributes to the existing literature by providing a comprehensive analytical model and steady-state calculations for frequency regulation of a power system including DR and VSG controls. Most of the available literature either considers DR [10,14–21,38,39] or virtual inertia [33,35–37,40] for the purpose of frequency control. The literature (e.g., [41,42]) that considers the presence of both has one or more of the following limitations: frequency regulation is not considered, simulation results for a specific case are provided instead of a general model of the power system, and the formulation for steady-state error is not provided.

The rest of the paper is organized as follows. In Section 2, a simple model of the conventional power system is appended by considering DR and VSG control loops for the frequency control analysis. The mathematical equations for frequency deviation and share of powers from DR, VSG, and conventional resources at steady-state are also developed in Section 2. In Section 3, simulation results are provided by considering DR and VSG controls. The conclusion of the paper and potential future work is provided in Section 4.

2. Development of the Proposed Model

Electrical power systems exhibit time-varying and highly nonlinear characteristics. However, the nature of dynamics affecting the frequency response is slow in comparison to rotor angle or voltage dynamics. Therefore, a widely accepted low-order linearized model is sufficient for frequency response analysis and control. A generalized model of a power system in the presence of load disturbance is presented by power balance equation as given in Equation (1) [1].

$$\Delta P_m(s) - \Delta P_d(s) = D\Delta f(s) + 2sH\Delta f(s) \tag{1}$$

where frequency deviation (Δf) is due to power mismatch ($\Delta P_m - \Delta P_d$), while D and H represent equivalent load-damping coefficient and inertia constant, respectively. In this equation, however, DR and virtual inertia are not included. A modified block diagram of a power system for the purpose of frequency control synthesis and analysis containing supplementary (or conventional), DR, and VSG control loops is shown in Figure 1. In the following subsections, DR and virtual inertia are modeled and added to the linear model of the electric power system.

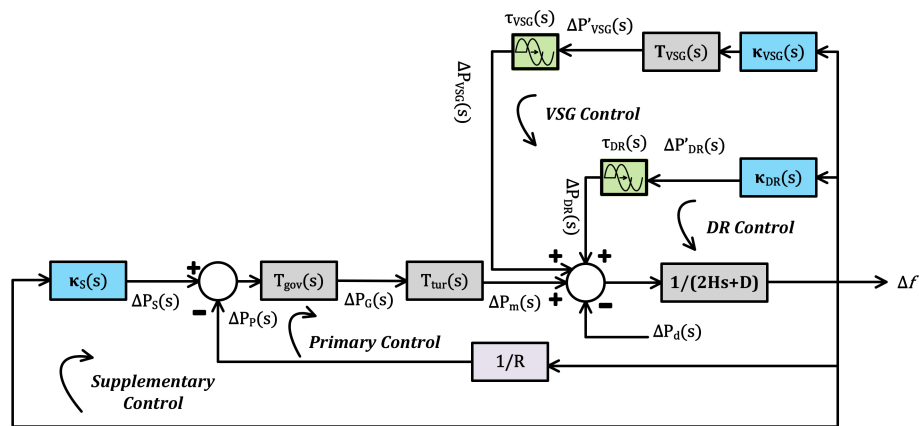


Figure 1. The block diagram of a power system for frequency response analysis including DR and VSG control loops.

2.1. Power System Model with DR

In addition to its application for long-term energy balance, DR can be effectively used for quick frequency regulation. The use of DR for the frequency regulation is simple to understand where a negative/positive frequency deviation requires turning off/on or reducing/increasing responsive loads. This will improve the real-power balance and hence the frequency profile. The control system shown in Figure 1 is redrawn in Figure 2 with emphasis on the effect of power disturbance (ΔP_d) on the system frequency.

Including DR control loop with the conventional control system, Equation (1) is transformed into Equation (2) where $\Delta P'_{DR}$ is a change in DR power. The negative (positive) frequency deviation will require turning off (on) a part of responsive loads to balance the real power supply and demand. In Equation (2), the delay in DR control loop is temporarily ignored. A binary indicator function χ_{DR} , which is availability indicator of DR control for frequency regulation, is introduced to maintain the general form of power balance equation. Its value is 1 if DR is available for frequency regulation, otherwise 0.

$$\Delta P_m(s) - \Delta P_d(s) + \chi_{DR}\Delta P'_{DR}(s) = D\Delta f(s) + 2sH\Delta f(s) \tag{2}$$

DR control is well-known for its fast response for frequency regulation in comparison to conventional control which requires, for example, change in valve/gate position [15,29]. The delay in DR control loop is primarily due to communication delay which depends upon communication

infrastructure itself. Further, system operators would also like to introduce some delay before the responsive loads respond to any frequency deviation. This model incorporates a time delay, $T_{d,DR}$, in DR control loop and the linearized transfer function of time delay using Padé approximation [43] is represented by $\tau_{DR}(s)$ in Figure 2. Thus, Equation (3) is obtained after considering time delay in DR loop.

$$\Delta P_m(s) - \Delta P_d(s) + \chi_{DR} \tau_{DR}(s) \Delta P'_{DR}(s) = D \Delta f(s) + 2sH \Delta f(s) \tag{3}$$

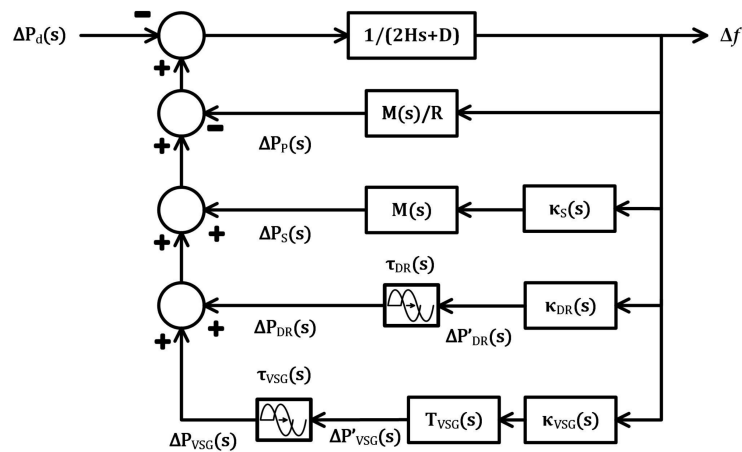


Figure 2. The modified representation of power system model relating frequency deviation to a power disturbance.

2.2. Power System Model with VSG

The concept behind a VSG is to mimic the dynamic properties of an actual synchronous generator for the power electronics-based RES units. The aim is to attain similar grid stability properties as that of a real synchronous generator. The main constituents of a VSG are ESS, a converter, and a control system, as shown in Figure 3. The nominal state of charge (SOC) of the energy storage is kept at slightly above or half of its nominal capacity in normal situations so that the VSG can inject or absorb power. When the ESS supplies power to the grid, it is in virtual generator state. On the other hand, the VSG works in virtual load mode when grid’s excess energy is stored in the ESS. Generally, the ranges of operating modes (i.e., virtual generator or virtual load mode) are dependent on the technology used for ESS. The selection of energy storage technology for VSG applications depends on the several parameters including the maximum power of the loads, rating of the controllable generation units, control delay and detection time, and average SOC during normal operation in the considered system [29,44].

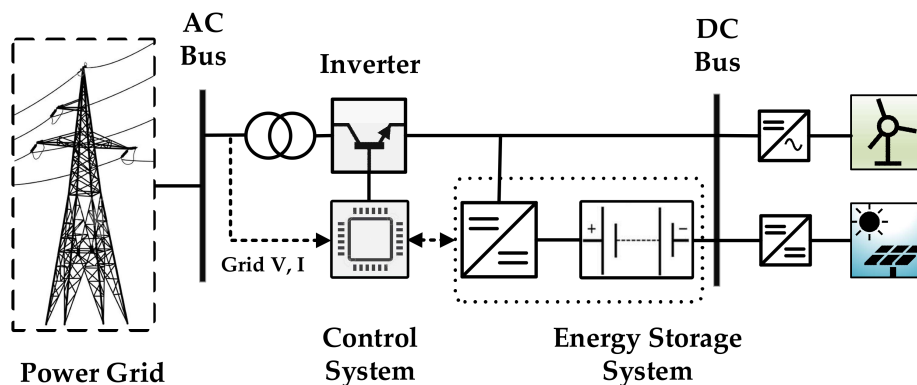


Figure 3. A typical structure of a virtual synchronous generator (VSG).

For the purpose of frequency response analysis and control, the output power of a VSG in the time domain is calculated by Equation (4) [29,45].

$$P_{VSG}(t) = P_{0,inv} + K_I \frac{d}{dt}(\Delta f(t)) + K_P \Delta f(t) + K_{SOC}(t) \delta_{SOC} \quad (4)$$

where $P_{0,inv}$ is the required primary power to or from the inverter and $\Delta f(t)$ is the difference between measured and reference frequency. The term K_I represents the inertia emulating characteristic of VSG and its value is proportional to the nominal apparent power of the generator. Mathematically, the higher value of K_I should result in the increased equivalent inertia of the VSG. However, in practical systems, inverter capacity and measurement accuracy define the limits of K_I . Practically, the value of K_I is chosen such that the maximum defined rate of change of frequency (ROCOF) causes the VSG to exchange its maximum power. The VSG will generate (absorb) power in accordance with the negative (positive) rate of change of frequency to make sure that the system frequency returns to its reference value at steady-state. The third term in the above equation serves as frequency droop part where K_p emulates the effects of damper winding of a real synchronous generator. The value of K_p is chosen such that VSG power is maximum when the frequency deviation reaches a predefined maximum limit. The last term in Equation (4) formulates the role of battery ESS where K_{SOC} and δ_{SOC} represent the battery's state of charge and charging coefficient, respectively. In this work, maximum ROCOF is considered as 1 Hz/s and maximum frequency deviation is set at 2.5 Hz [29,45].

The transfer function of frequency deviation with respect to change in VSG power is shown in Equation (5). In this equation, only inverter dynamics are considered and the effect of the battery ESS is neglected supposing the sufficient charging/discharging capacity of the batteries.

$$T_{VSG}(s) = \frac{1}{K_I s + K_P} \quad (5)$$

This transfer function will be used in subsequent sections to complete the model of the power system for frequency control analysis. It is notable that when viewed from the grid side, the electrical facade of an electrical VSG is similar to that of an electromechanical SG. The only difference is the higher frequency noise due to switching operation of power transistors of the inverter [40].

Considering the VSG control loop in Figure 2, and neglecting the DR control for the moment, Equation (6) includes VSG control with the conventional control.

$$\Delta P_m(s) - \Delta P_d(s) + \chi_{VSG} \tau_{VSG}(s) \Delta P'_{VSG}(s) = D \Delta f(s) + 2sH \Delta f(s) \quad (6)$$

where χ_{VSG} is the indicator function of the availability of VSG power, τ_{VSG} is the delay in the VSG loop, and $\Delta P'_{VSG}$ is the VSG power.

2.3. Power System Model with DR and VSG

Considering both DR and VSG are available (i.e., $\chi_{DR} = \chi_{VSG} = 1$), Equation (7) is obtained after solving Equations (3) and (6) for Δf ,

$$\Delta f(s) = \frac{1}{(2Hs + D)} [\Delta P_m(s) - \Delta P_d(s) + \tau_{DR} \Delta P'_{DR}(s) + \tau_{VSG} \Delta P'_{VSG}(s)] \quad (7)$$

or

$$\Delta f(s) = \frac{1}{(2Hs + D)} [\Delta P_m(s) - \Delta P_d(s) + \Delta P_{DR}(s) + \Delta P_{VSG}(s)] \quad (8)$$

where ΔP_{DR} and ΔP_{VSG} represent the change in DR and VSG powers after considering the time delays as given in Equations (9) and (10). It is clear that, at steady-state, ΔP_{DR} and ΔP_{VSG} are equal to $\Delta P'_{DR}$ and $\Delta P'_{VSG}$, respectively.

$$\Delta P_{DR}(s) = \tau_{DR}(s) \Delta P'_{DR}(s) \quad (9)$$

$$\Delta P_{VSG}(s) = \tau_{VSG}(s) \Delta P'_{VSG}(s) \quad (10)$$

In Figure 2, $M(s)$ represents the generalized transfer function of a prime-mover that runs the synchronous generator. Mathematically,

$$M(s) = T_{gov}(s) \cdot T_{tur}(s) \quad (11)$$

There are different transfer functions for different types of turbines, as mentioned in Equation (12) [46].

$$T_{tur}(s) = \begin{cases} \frac{1}{T_t s + 1}, & \text{non-reheat turbine} \\ \frac{c T_r s + 1}{(T_t s + 1)(T_r s + 1)}, & \text{reheated turbine} \\ \frac{1 - T_w s}{(0.5 T_w s + 1)}, & \text{hydro turbine} \end{cases} \quad (12)$$

2.4. Steady-State Evaluation of the Proposed Model

Considering the power disturbance as a step disturbance, its Laplace Transformation is provided in Equation (13):

$$\Delta P_d(s) = \frac{\Delta P_d}{s} \quad (13)$$

Equation (8) can be re-written as:

$$\Delta f(s) = \frac{1}{N(s)} [M(s) \cdot \Delta P_S(s) + \Delta P_{DR}(s) + \Delta P_{VSG}(s)] - \frac{1}{N(s)} \Delta P_d(s) \quad (14)$$

where

$$N(s) = 2Hs + D + \frac{M(s)}{R} \quad (15)$$

Applying the final value theorem and considering Equations (9) and (10), we get:

$$\Delta f_{SS} = \lim_{s \rightarrow 0} s \cdot f(s) = \frac{\Delta P_{S,SS} + \Delta P_{DR,SS} - \Delta P_d}{N(0)} \quad (16)$$

where

$$\Delta P_{S,SS} = \lim_{s \rightarrow 0} s \cdot M(s) \cdot \Delta P_S(s) \quad (17)$$

and

$$\Delta P_{DR,SS} = \lim_{s \rightarrow 0} s \cdot \Delta P_{DR}(s) \quad (18)$$

$$\Delta P_{VSG,SS} = \lim_{s \rightarrow 0} s \cdot \Delta P_{VSG}(s) \quad (19)$$

$$N(0) = D + \frac{M(0)}{R} = D + \frac{1}{R} \quad (20)$$

The term $N(0)$ in Equation (20) represents the system frequency response characteristics [15]. Finally, the steady-state frequency deviation is calculated using Equation (21) as follows:

$$\Delta f_{SS} = \frac{\Delta P_{S,SS} + \Delta P_{DR,SS} + \Delta P_{VSG} - \Delta P_d}{D + \frac{1}{R}} \quad (21)$$

As indicated by Equation (21), steady-state frequency deviation can be zero only if one or more of the three powers (supplementary, DR, and VSG) are sufficiently available to balance the disturbance (ΔP_d). Equation (21) indicates that DR and/or VSG can also be utilized to regulate the frequency in

addition to the supplementary control, thus providing the system operator with improved capability of frequency regulation.

If K is the total control effort to balance the effect of ΔP_d , then it must be distributed among three controllers (i.e., supplementary, DR, and VSG) according to Equation (22).

$$K = K_S + K_{DR} + K_{VSG} \quad (22)$$

Power system operator has an extra degree of freedom to optimally decide the share from each control loop to regulate the system frequency in a timely and cost-effective manner. If the shares of DR, VSG, and supplementary controls are ε , ζ , and γ , respectively, such that:

$$\gamma = 1 - \varepsilon - \zeta \quad (23)$$

then, the contribution of DR control is given in Equation (24):

$$K_{DR} = \varepsilon \cdot K \quad (24)$$

Equation (25) formulates the role of VSG control as:

$$K_{VSG} = \zeta \cdot K \quad (25)$$

Finally, the supplementary control has to provide the rest of control effort according to Equation (26) as follows:

$$K_S = (1 - \varepsilon - \zeta) \cdot K \quad (26)$$

Consequently, the steady-state contribution of each participant to mitigate the steady-state frequency deviation is distributed as given by Equations (27)–(29):

$$\Delta P_{DR,SS} = \varepsilon \cdot \Delta P_L \quad (27)$$

$$\Delta P_{VSG,SS} = \zeta \cdot \Delta P_L \quad (28)$$

$$\Delta P_{S,SS} = (1 - \varepsilon - \zeta) \cdot \Delta P_L \quad (29)$$

It is notable that steady-state values depend on the share between the supplementary control (γ), DR control (ε), and VSG control (ζ) which is determined by the system operator in negotiation with customers. Multiple factors (e.g., the network condition, the real-time electricity price, capacity of ESS, etc.) affect the values of ε , ζ , and γ . The proposed model maintains the general form of a single-area power system model where the absence of DR and VSG will result in the traditional frequency control model.

3. Simulation Results

This section demonstrates various key features of the developed model. In fact, whenever a new model or technique is developed, a set of simulations demonstrating the role of important parameters is performed to assess the performance of proposed model or technique. Several simulations were performed to analyze the effects of load disturbance on the system frequency response considering various parameters such as control share of DR and VSG, delay times, and frequency deadbands. For impartial comparison and to avoid mathematical complexities, classical PID control has been implemented in all simulated scenarios. The controllers were tuned using Control System Toolbox of MATLAB/Simulink, and the values of P, I, and D control actions are provided in Appendix A. Further, the simulations have been performed on different systems with slow and fast dynamics to assess the performance of the developed model in a generalized grid structure. The system parameters for the two power grids are provided in Table 1. Only the graphical results for the system with fast dynamics

are shown here as the obtained results exhibit the consistent behavior of proposed model towards system frequency response in both cases. The power system base is 100 MW with a peak power of 85 MW for conventional and 15 MW for wind generation. The proposed model is validated by simulating the effects of load disturbance in following cases: only DR, only VSG, DR and VSG, and DR with VSG in the presence of unregulated wind generation. The dynamic effects of DR and VSG controls on the system frequency response are discussed in the dedicated subsections. Further, the contribution or change in turbine/DR/VSG powers is also shown to verify that these are according to the proposed model and equations provided in Section 2. In all simulation cases, step load disturbance of 0.05 p.u is applied at $t = 6$ s, and detailed descriptions of the simulation scenarios are provided in Tables 2–5.

Table 1. Parameters of test systems with slow and fast dynamics [15].

Parameter	System with Fast Dynamics (System-I)	System with Slow Dynamics (System-II)
R	3 Hz/p.u	2.4 Hz/p.u
D	0.015 p.u/Hz	0.0083 p.u/Hz
$2H$	0.15 p.u s	3 p.u s
T_t	0.4 s	0.8 s
T_g	0.08 s	0.3 s
P_d	0.05 p.u	0.05 p.u
Deadband (Governor)	± 0.036 Hz	± 0.036 Hz
GRC (Turbine)	± 0.1 p.u	± 0.1 p.u

3.1. DR Control

The impacts of three important parameters of DR control loop (i.e., DR control share (ϵ), delay times ($T_{d,DR}$), and frequency deadband in DR control loop ($f_{DR,DB}$)) on system frequency response are presented here. Table 2 shows the various simulation scenarios and parameter setting for each case.

Table 2. DR control: simulation scenarios and parameter setting.

Scenario	Case No	Setting	Other Parameters
Effect of DR Control Share (ϵ)	1	$\epsilon = 0$ (No DR)	
	2	$\epsilon = 0.1$	$\Delta P_d(s) = 0.05$ p.u
	3	$\epsilon = 0.2$	$f_{DR,DB} = 0.05\%$
	4	$\epsilon = 0.3$	$T_{d,DR} = 0.1$ s
	5	$\epsilon = 0.5$	
Effect of Delay Times ($T_{d,DR}$)	1	No DR	
	2	$T_{d,DR} = 0.0$ s	$\Delta P_d(s) = 0.05$ p.u
	3	$T_{d,DR} = 0.2$ s	$\epsilon = 0.3$
	4	$T_{d,DR} = 0.5$ s	$f_{DR,DB} = 0.1\%$
	5	$T_{d,DR} = 0.8$ s	
Effect of Frequency Deadband ($f_{DR,DB}$)	1	No DR	
	2	$f_{DR,DB} = 0.0\%$	$\Delta P_d(s) = 0.05$ p.u
	3	$f_{DR,DB} = 0.05\%$	$\epsilon = 0.4$
	4	$f_{DR,DB} = 0.1\%$	$T_{d,DR} = 0.1$ s
	5	$f_{DR,DB} = 0.5\%$	

3.1.1. Effect of DR Control Share (ϵ)

In this simulation study, the effects of DR control share (ϵ) on system frequency response are provided. Ranging from purely conventional control (i.e., no DR control share, $\gamma = 100\%$ and $\epsilon = 0\%$) to 50% DR control share, the frequency deviation for each case is shown in Figure 4a. The following inferences can be made from the results:

- The participation of DR control results in improved frequency response.

- The higher value of ε yields better results, in general. The higher value of ε indicates that more consumers are willing to take part in DR for frequency regulation. As shown in Figure 4a, the higher DR contribution results in improved transient behavior and settling time (e.g., $\varepsilon = 50\%$ results in 13.3% lesser maximum frequency deviation as compared to $\varepsilon = 0\%$).
- On the other hand, the lower the values of ε , the closer the frequency response to the conventional control.
- The steady-state values of DR and turbine powers are conforming to the steady-state model developed in Section 2 and their values are according to Equations (27)–(29). For example, in Case 3, $\varepsilon = 20\%$ results in $\Delta P_{DR,SS} = 0.2 \times 0.05 = 0.01$ p.u and $\Delta P_{S,SS} = (1 - 0.2) \times 0.05 = 0.04$ p.u, as shown in Figure 4b–d.

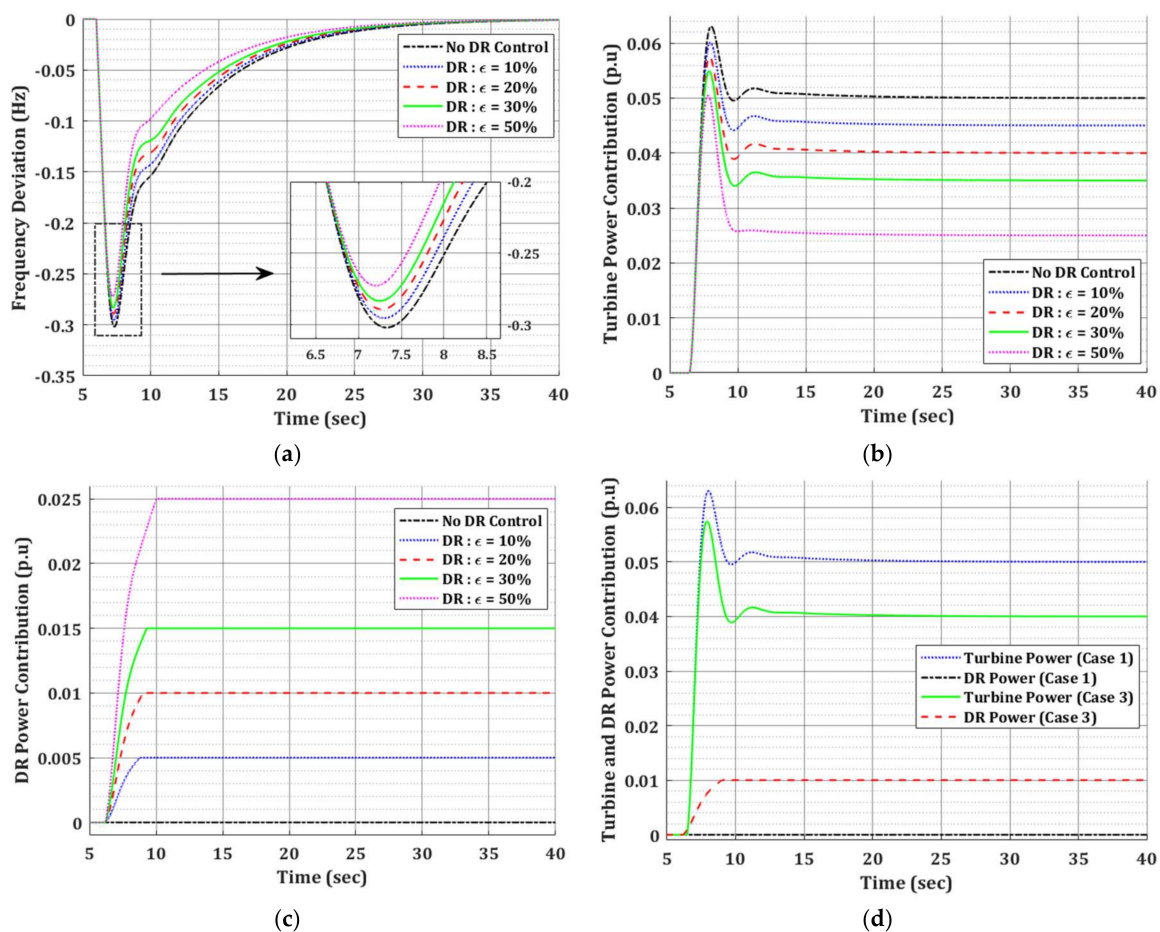


Figure 4. Effect of DR control share (ε) on various system parameters under load disturbance: (a) system frequency response; (b) change in turbine power (p.u); (c) change in DR power (p.u); and (d) change in turbine and DR powers (p.u) for selected cases.

3.1.2. Effect of Delay Times ($T_{d,DR}$)

The time delays appear either due to communication latency or intentionally introduced to compensate momentary changes. In the proposed model, the system operator can introduce a time delay in the DR control loop to let the supplementary control play its role first so that consumer's comfort level is minimally disturbed. In this simulation study, the effects of time delays in DR loop on system frequency response are analyzed. The simulation results are presented in Figure 5 for various cases detailed in Table 2. Figure 5a shows that better results are obtained if the time delay is small (e.g., $T_{d,DR} = 0.2$ s). Such time delays are achievable in smaller systems with fast communication

infrastructure. For widespread power systems, the increased time delay (e.g., $T_{d,DR} = 0.8$ s in Case 5) does not allow DR control system to exceptionally outperform and the system frequency response is nearly similar to the response with conventional control. The promising thing for DR control, however, in the context of a widespread large power system is the slow dynamic response of power generation unit due to the higher inertia of bigger machines and generation rate constraints (e.g., System-II in Table 1). In such scenarios, communication infrastructure with even higher latencies can allow DR control perform very well in comparison to slower conventional control.

The change in turbine and DR powers are shown in Figure 5b–d where the steady-state values conform to Equations (27)–(29). The value of DR control share is fixed in this study (i.e., $\varepsilon = 30\%$) and hence $\Delta P_{DR,SS} = 0.3 \times 0.05 = 0.015$ p.u and $\Delta P_{S,SS} = (1 - 0.3) \times 0.05 = 0.035$ p.u.

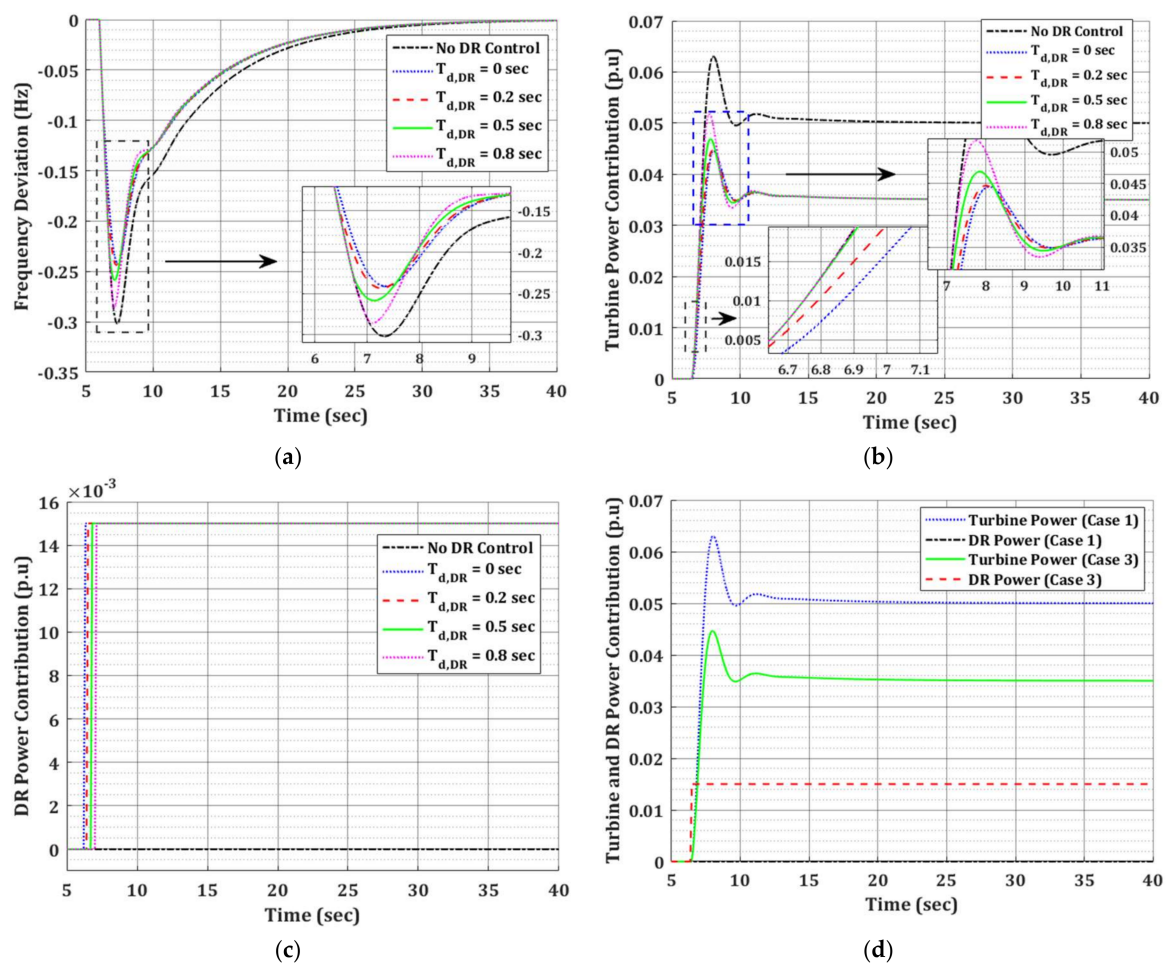


Figure 5. Effect of delay times ($T_{d,DR}$) on various system parameters under load disturbance: (a) system frequency response; (b) change in turbine power (p.u); (c) change in DR power (p.u); and (d) change in turbine and DR power (p.u) for selected cases.

3.1.3. Effect of Frequency Deadband ($f_{DR,DB}$)

Owing to the reasons of momentary changes, measurement and calculation errors, better sensitivity, and physical limits, there are regions, known as deadbands, in which frequency variation does not affect the control output of frequency controllers. Intuitively, larger deadbands degrade system performance, and very tight deadbands result in increased operation and maintenance cost. Thus, the power generation units are designed and operated following industry standards. For example, IEEE Std. 122-1991 recommends the maximum value of deadband as 0.06% for the governors of large-size conventional steam turbines [47].

The simulation results presented in this section analyze the effects of frequency deadband provided in DR control loop as it is often desired not to disturb the loads during small frequency deviations. The provision of deadband can also take care of frequency fluctuations caused by RES such as wind. Figure 6a shows system frequency response for step load disturbance with and without DR control under various frequency deadbands in DR control loop. As expected, Case 2 ($f_{DR,DB} = 0\%$) provided the best simulation results anyhow; it has drawbacks in practical applications. The deadband in Case 3 ($f_{DR,DB} = 0.05\%$) is very close to the deadband in supplementary control (0.06% or 0.036 Hz as mentioned in Table 1), but the frequency response is better. Case 4 ($f_{DR,DB} = 0.1\%$) is more interesting, as it has practical appeal (i.e., do not let the loads be disturbed unless it is urgent to do so) and results in lesser frequency deviation and settling time as compare to Case 1. There is no difference between frequency profile of Case 1 (No DR Control) and Case 5 ($f_{DR,DB} = 0.5\%$). The latter case requires at least 0.3 Hz (0.5% of 60 Hz) frequency deviation to initiate DR control which does not occur in this case. Hence, there is no effect on system frequency and no contribution from DR power, as shown in Figure 6c.

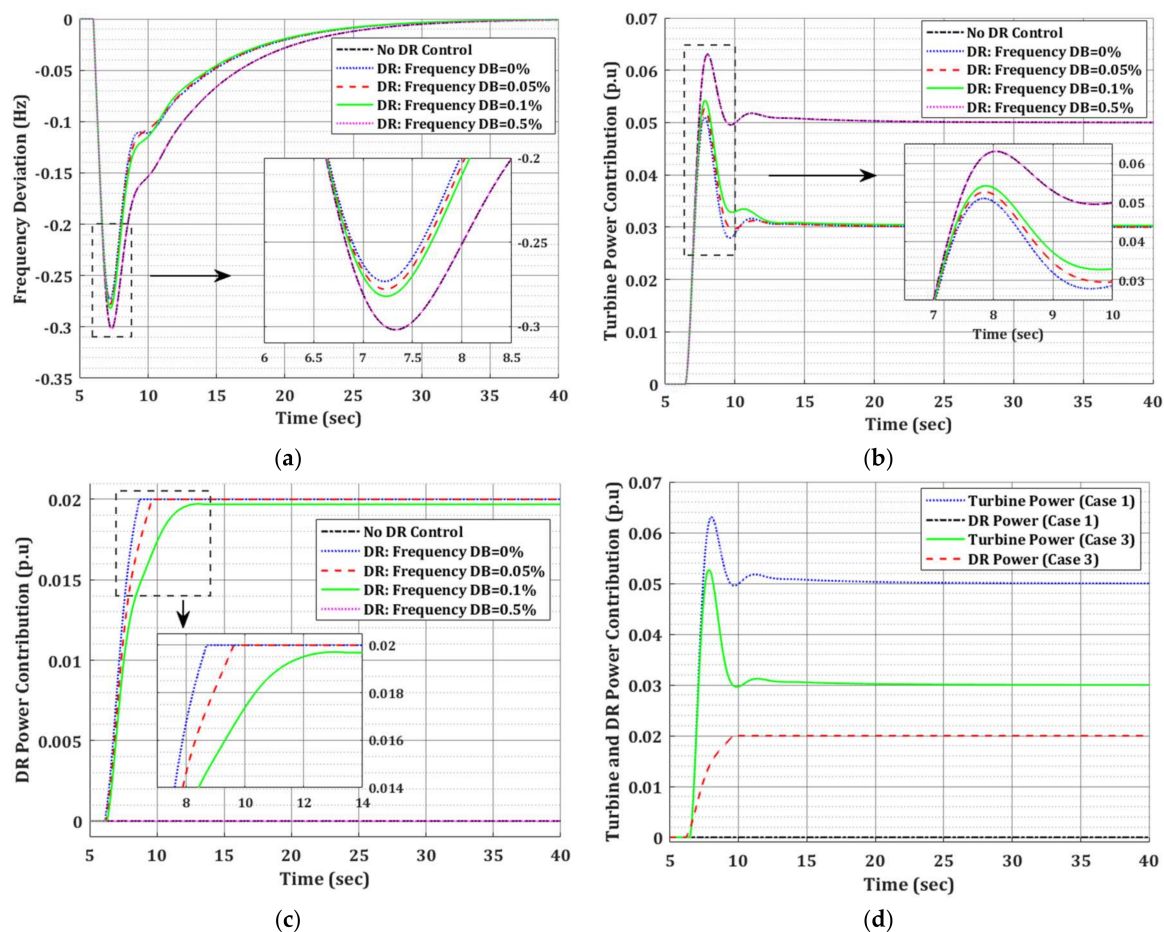


Figure 6. Effect of frequency deadband ($f_{DR,DB}$) on various system parameters under load disturbance: (a) system frequency response; (b) change in turbine power (p.u); (c) change in DR power (p.u); and (d) change in turbine and DR power (p.u) for selected cases.

3.2. VSG Control

This section presents simulation results of including VSG control in the system model. The impact of VSG control share (ζ) and frequency deadband ($f_{VSG,db}$) is analyzed under various simulation conditions, as detailed in Table 3.

Table 3. VSG control: simulation scenarios and parameter setting.

Scenario	Case No	Setting	Other Parameters
Effect of VSG Control Share (ζ)	1	No VSG	
	2	$\zeta = 0.1$	$\Delta P_d(s) = 0.05$ p.u
	3	$\zeta = 0.2$	$f_{VSG,DB} = 0.05\%$
	4	$\zeta = 0.3$	$T_{d,VSG} = 0.1$ s
	5	$\zeta = 0.5$	
Effect of Frequency Deadband ($f_{VSG,DB}$)	1	No VSG	
	2	$f_{VSG,DB} = 0.0\%$	$\Delta P_d(s) = 0.05$ p.u
	3	$f_{VSG,DB} = 0.05\%$	$T_{d,VSG} = 0.1$ s
	4	$f_{VSG,DB} = 0.1\%$	
	5	$f_{VSG,DB} = 0.5\%$	

3.2.1. Effect of VSG Control Share (ζ)

The effects of changing VSG control share (ζ) from $\zeta = 0\%$ to $\zeta = 50\%$ on system frequency response under load disturbance are shown in Figure 7. The following points are observed in this simulation study:

- The VSG control loop improved overall frequency response in proportion to the VSG control share (ζ). The value of VSG control share (ζ) is determined by the system operator considering VSG rating and other parameters.
- The higher VSG contribution results in improved system frequency response (e.g., in Case 5, $\zeta = 50\%$ results in 33.3% less maximum frequency deviation when compared with no VSG control).
- In Figure 7b–d, the steady-state values of change in turbine and VSG powers are shown, which conform to Equations (27)–(29) (e.g., for Case 3, $\zeta = 20\%$ results in $\Delta P_{VSG,SS} = 0.2 \times 0.05 = 0.01$ p.u and $\Delta P_{S,SS} = (1 - 0.2) \times 0.05 = 0.04$ p.u, as shown in Figure 7b–d).

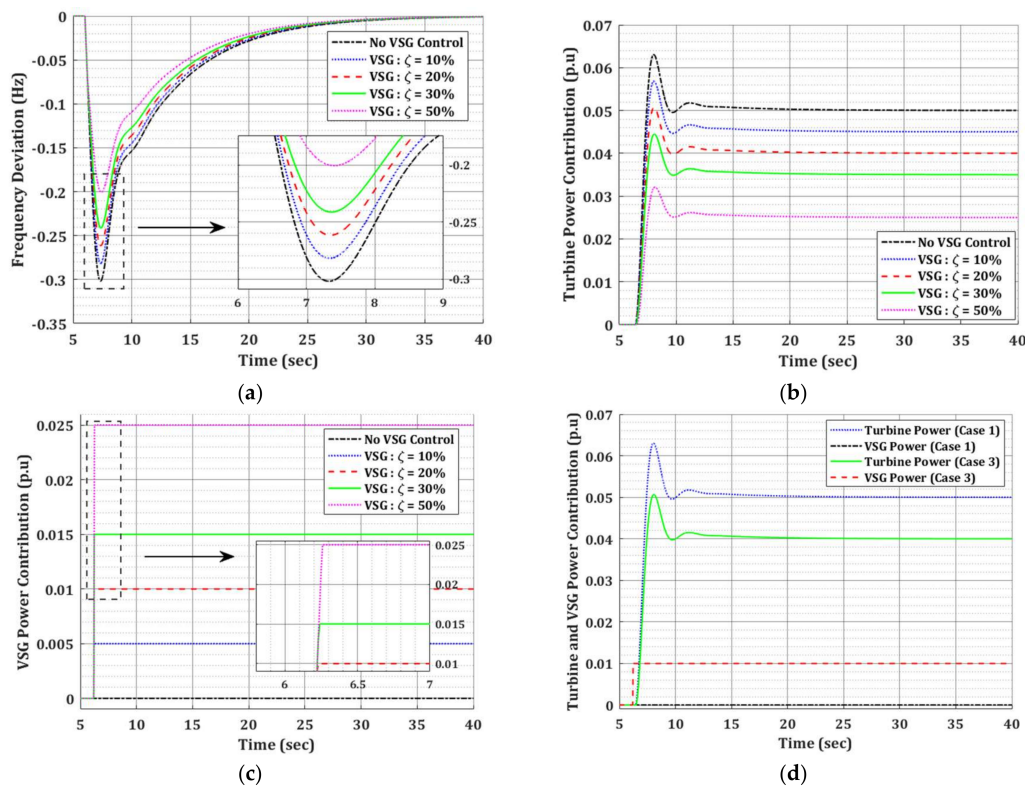


Figure 7. Effect of VSG control share (ζ) on various system parameters under load disturbance: (a) system frequency response; (b) change in turbine power (p.u); (c) change in VSG power (p.u); and (d) change in turbine and VSG power (p.u) for selected cases.

3.2.2. Effect of Frequency Deadband ($f_{VSG,DB}$)

The simulation results presented in Figure 8 analyze the effects of providing frequency deadband in VSG control loop. The important observations are summarized as follows:

- The steady-state values of change in turbine and VSG powers are shown in Figure 8b–d, which conform to Equations (27)–(29).
- Considering Case 5, the magnitude of frequency deviation exceeds the higher value of frequency deadband ($f_{VSG,DB} = 0.5\% = 0.3$ Hz) at $t \approx 7.4$ s and there is quick but small contribution from VSG power at that instance. This contribution dies soon, as the magnitude of frequency deviation falls below 0.3 Hz (Figure 8a,c).

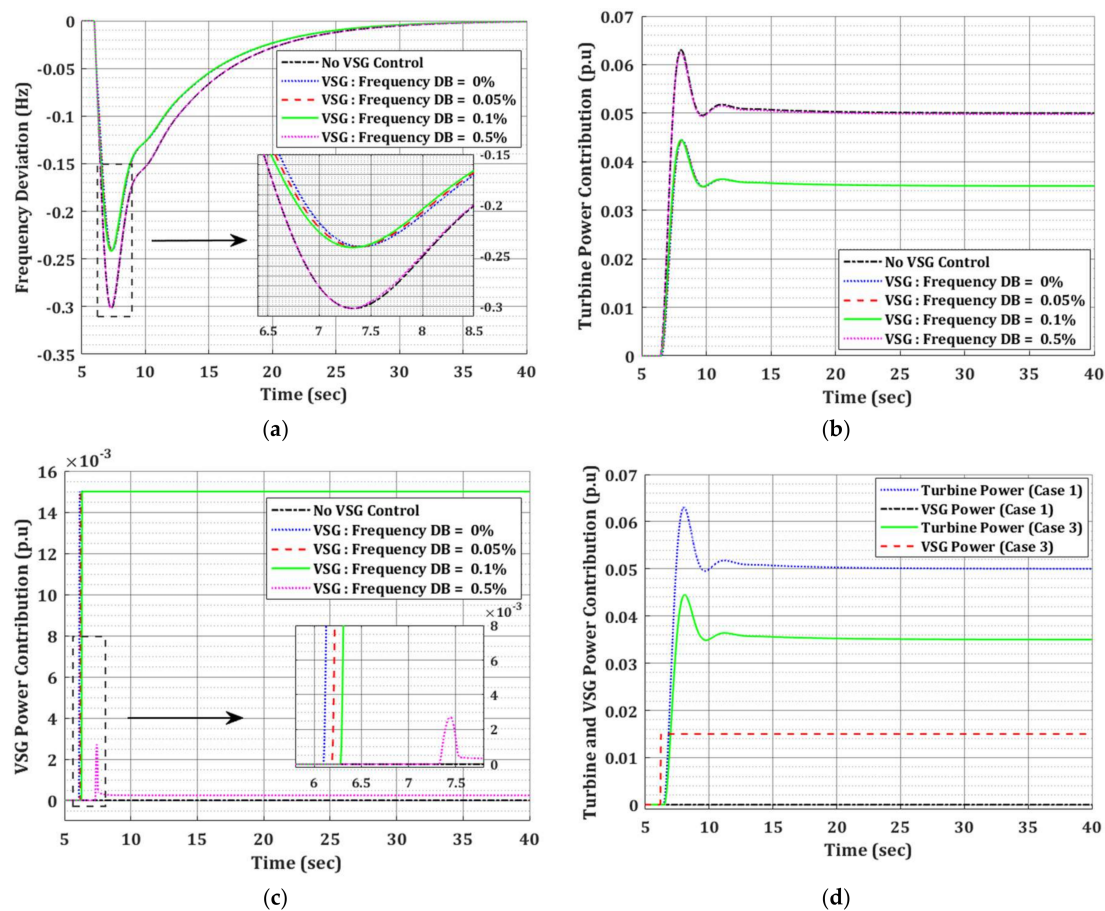


Figure 8. Effect of frequency deadband ($f_{VSG,DB}$) on various system parameters under load disturbance: (a) system frequency response; (b) change in turbine power (p.u); (c) change in VSG power (p.u); and (d) change in turbine and VSG power (p.u) for selected cases.

3.3. DR and VSG Control

After presenting the roles of DR and VSG control loops individually, it is time to demonstrate their combined effectiveness in frequency control of a power system. In this section, five cases are considered, as summarized in Table 4, to analyze the effect of various parameters in frequency control loops. The results are presented in Figure 9. Case 1 does not consider DR and VSG in the frequency control, while the four other cases consider either DR or VSG, or both. The following points are observed from this simulation study:

- Case 4, in which both DR and VSG controls have an equal share, shows 17.8% less frequency deviation as compared to Case 1. In Case 5, only VSG control plays a role because the DR control has higher frequency deadband ($f_{DR,DB} = 0.5\% = 0.3$ Hz).
- The steady-state contribution of powers from the turbine, DR and VSG, shown in Figure 9b–d, are in accordance with Equations (27)–(29). The contribution from turbine power is 0.04 p.u in Case 5 because DR control does not play its role due to higher frequency deadband (i.e., $\gamma = 1 - \epsilon - \zeta = 1 - 0 - 0.2 = 0.8$ and $\Delta P_{S,SS} = 0.8 \times 0.05 = 0.04$ p.u).

Table 4. DR and VSG control: simulation scenarios and parameter setting.

Scenario	Case No.	Setting	Other Parameters
Conventional control only	1	$\epsilon = 0, \zeta = 0$	$\Delta P_d(s) = 0.05$ p.u $f_{DR,DB} = f_{VSG,DB} = 0.01\%$ $T_{d,DR} = T_{d,VSG} = 0.1$ s
Only DR control added	2	$\epsilon = 0.4, \zeta = 0$	
Only VSG control added	3	$\epsilon = 0, \zeta = 0.4$	
DR and VSG controls added	4	$\epsilon = 0.2, \zeta = 0.2$	
DR and VSG controls added with $f_{DR,DB} = 0.5\%$	5	* $\epsilon = 0.2, \zeta = 0.2$	

* For Case 5 only, $f_{DR,DB} = 0.5\%$.

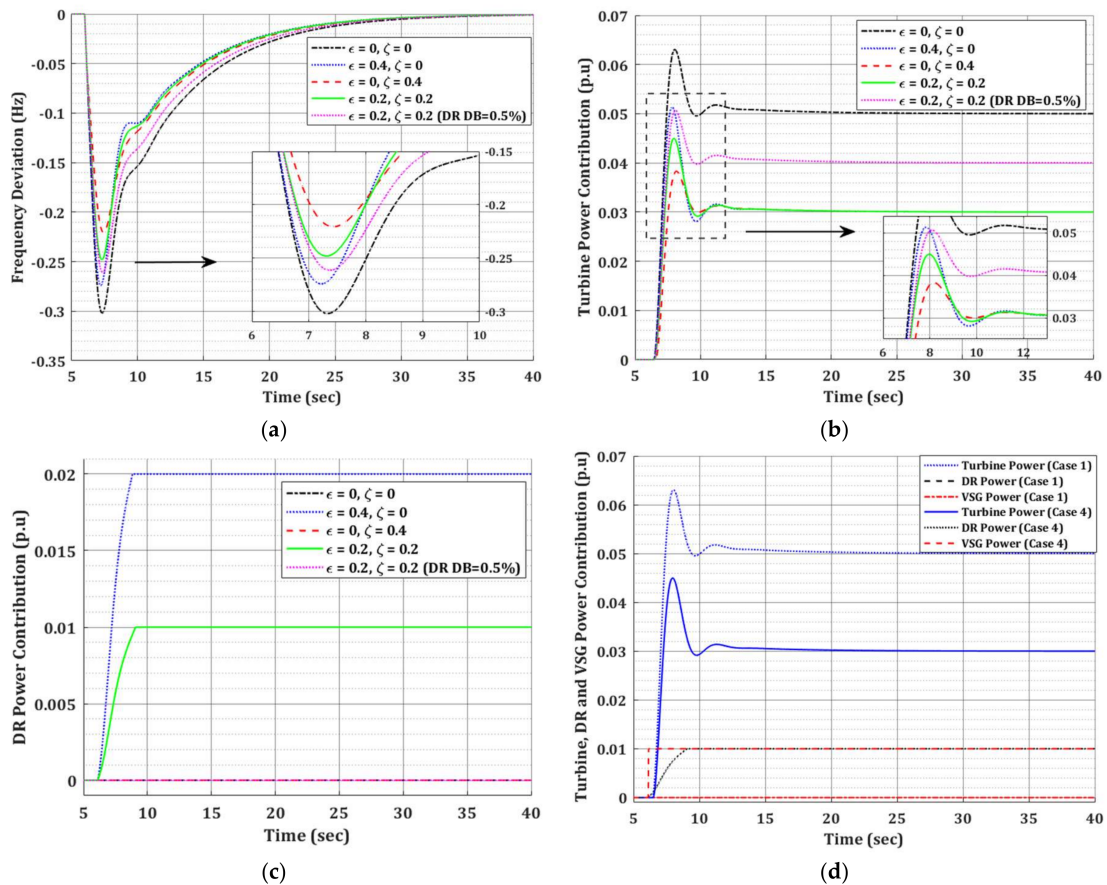


Figure 9. Effect of DR and VSG control on various system parameters under load disturbance: (a) system frequency response; (b) change in turbine power (p.u); (c) change in DR power (p.u); and (d) change in turbine, DR and VSG power (p.u) for selected cases.

3.4. DR and VSG Control in the Presence of Unregulated Wind Generation

In this section, the effects of unregulated wind generation on system frequency response is provided when both the DR and the VSG control loops are present in the system. The model of wind power for the purpose of frequency control is provided in Appendix B [37]. The study comprises five

simulation cases, including a case of high wind speed, as detailed in Table 5. The simulation results are shown in Figure 10 and important observations are summarized as follows:

- In Case 1, when there is no contribution from DR and VSG loops, the supplementary control accommodates the variations in wind generation.
- The increased wind generation can cause positive frequency deviation and the VSG control is supposed to absorb power during such scenarios. This is reflected in Figure 10d at $t < 6$ s.
- For higher wind generation, as in Case 5, the magnitude of power fluctuation is higher. This results in frequency variation even in steady-state ($t = 25\text{--}40$ s). One of the reasons of higher fluctuation is the fact that controllers in supplementary, DR and VSG control loops were not designed to handle the large fluctuations in wind power. In other words, an appropriately designed robust control system is required to diminish the steady-state error caused by intermittent wind generation.
- The steady-state contribution of powers from the turbine, DR and VSG are shown in Figure 10b–d,f, and conform to Equations (27)–(29).

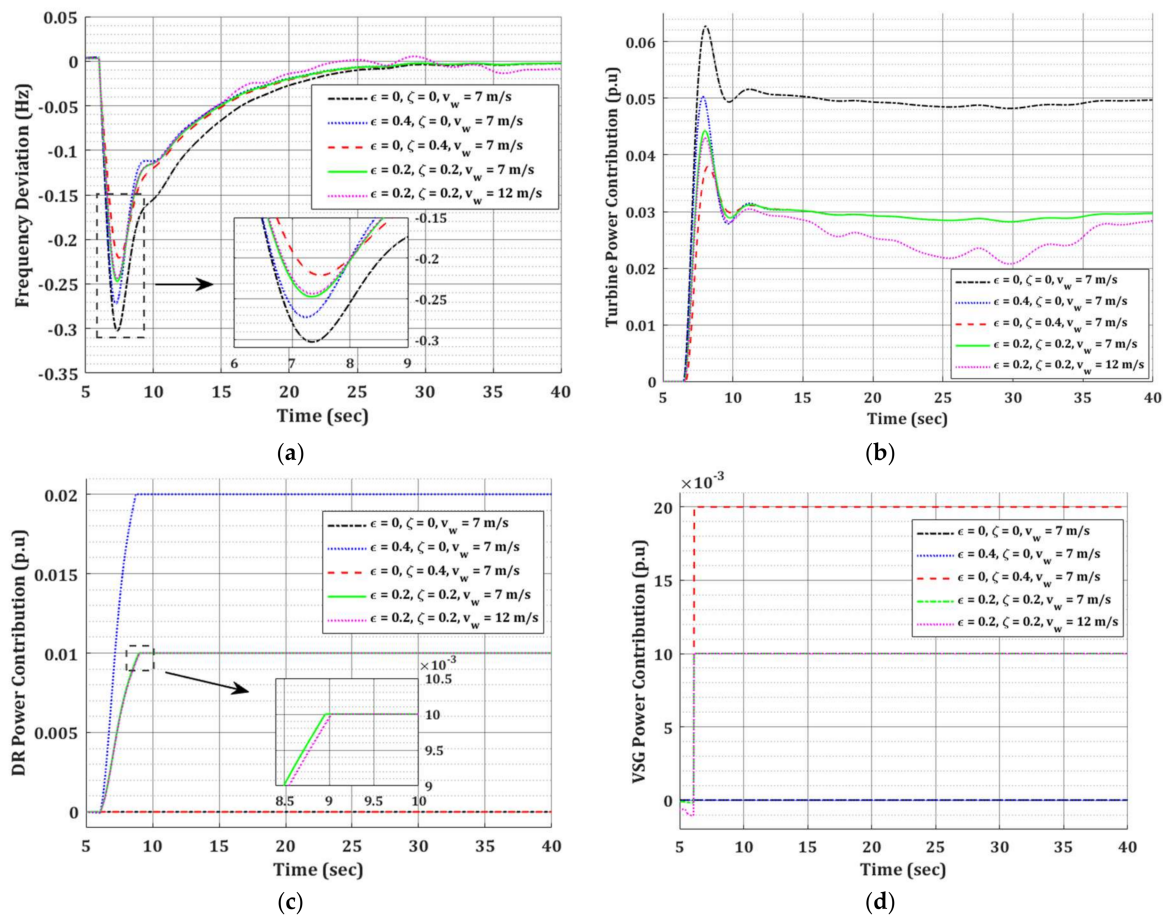


Figure 10. Cont.

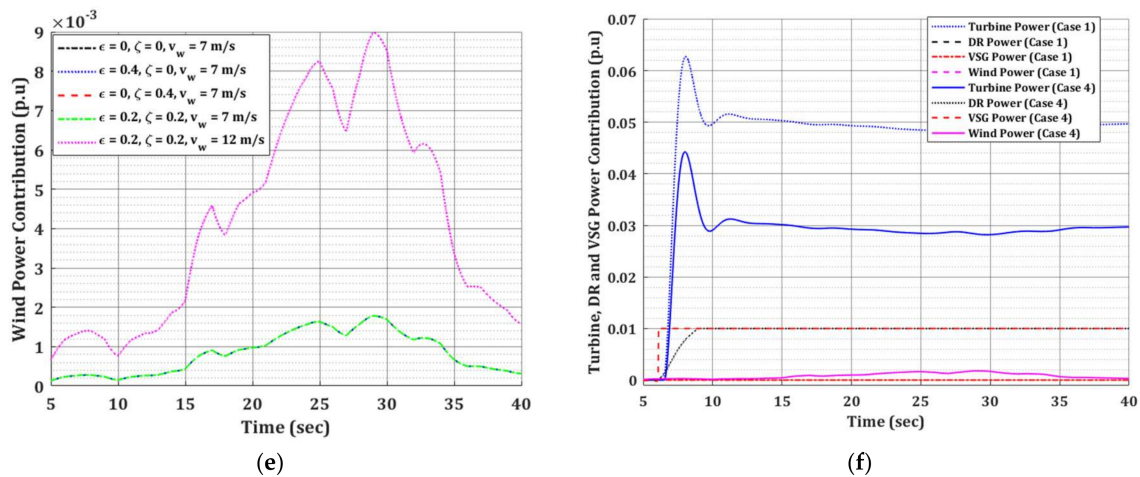


Figure 10. Effect of DR and VSG control on various system parameters under load disturbance in the presence of unregulated wind generation: (a) system frequency response; (b) change in turbine power (p.u); (c) change in DR power (p.u); (d) change in VSG power (p.u); (e) change in wind power (p.u); and (f) change in turbine, DR and VSG power (p.u) for selected cases.

Table 5. DR and VSG control in the presence of unregulated wind generation: simulation scenarios and parameter setting.

Scenario	Case No.	Setting	Other Parameters
Effect of unregulated wind generation	1	$\epsilon = 0, \zeta = 0, v_{w,av} = 7 \text{ m/s}$	$\Delta P_d(s) = 0.05 \text{ p.u}$ $f_{DR,DB} = f_{VSG,DB} = 0.005\%$ $T_{d,DR} = T_{d,VSG} = 0.01 \text{ s}$
	2	$\epsilon = 0.4, \zeta = 0, v_{w,av} = 7 \text{ m/s}$	
	3	$\epsilon = 0, \zeta = 0.4, v_{w,av} = 7 \text{ m/s}$	
	4	$\epsilon = 0.2, \zeta = 0.2, v_{w,av} = 7 \text{ m/s}$	
	5	$\epsilon = 0.2, \zeta = 0.2, v_{w,av} = 12 \text{ m/s}$	

4. Conclusions

The modern power grid has an increasing penetration of responsive loads and RES coupled with ESS. There has been limited work on analyzing their combined effect on system frequency response. In this paper, starting from a basic model of an electric power system, a comprehensive model of the electric power system including DR and VSG has been provided for the purpose of frequency response analysis and control. Model has been made as general as possible by including indicator functions and time delays. Further, formulation of DR and VSG control shares and their role in steady-state frequency control is mathematically provided and validated by simulation results. The presence of DR and/or VSG controls provide the system operator with additional capabilities for frequency regulation with minimum time delays. The distribution of power shares among supplementary, DR, and VSG control can be optimized under various constraints and could be a motivating topic for future research. Similarly, modifying power system inertia (H) to accommodate the role of the VSG, instead of adding a separate control loop, could also lead to interesting results.

Acknowledgments: This work was supported by the National Research Foundation of Korea (NRF) grant funded by the Korean Government (MSIP) (No. 2015R1A2A1A10052459).

Author Contributions: Muhammad Saeed Uz Zaman conceived the idea and did preliminary work. Chul-Hwan Kim provided guidelines necessary to complete the work. Zunaib Maqsood Haider provided clear ideas for using the DR concept for frequency regulation. Syed Basit Ali Bukhari helped in simulating the experiments and during paper writing. Raza Haider, Khalid Mousa Hazazi, and Chul-Hwan Kim analyzed the results, reviewed the paper, and directed significant improvements. Muhammad Saeed Uz Zaman wrote the paper.

Conflicts of Interest: The authors declare no conflict of interest.

Abbreviations

D	Damping coefficient of the system
$f_{DR,DB}$	Frequency deviation deadband for DR control
$f_{VSG,DB}$	Frequency deviation deadband for VSG control
H	Inertia constant
R	Droop characteristics
$T_{d,DR}$	Delay in DR control loop (s)
$T_{d,VSG}$	Delay in virtual synchronous generator control loop (s)
T_g	Time constant of governor
T_t	Time constant of non-reheat turbine
T_w	Time constant of hydro turbine
γ	share of supplementary control for frequency regulation
ε	share of DR control for frequency regulation
ζ	share of VSG control for frequency regulation
K	Total control effort to minimize frequency deviation
K_S	Control effort provided by supplementary control to minimize frequency deviation
K_{DR}	Control effort provided by DR control to minimize frequency deviation
K_{VSG}	Control effort provided by VSG control to minimize frequency deviation
$\kappa_{DR}(s)$	DR controller
$\kappa_{VSG}(s)$	Virtual synchronous generator controller
$\tau_{DR}(s)$	linearized transfer function of delay in DR control loop
$\tau_{VSG}(s)$	linearized transfer function of delay in VSG control loop
χ_{DR}	Availability indicator of DR control for frequency regulation
χ_{VSG}	Availability indicator of VSG control for frequency regulation
$\Delta f(s)$	Change in frequency
Δf_{SS}	Steady-state frequency deviation
$\Delta P_d(s)$	Change in load (Load disturbance)
$\Delta P_{DR}(s)$	Change in DR power
$\Delta P_{DR,SS}$	Share of DR power at steady-state
$\Delta P_m(s)$	Change in turbine's power
$\Delta P_S(s)$	Change in power due to supplementary control
$\Delta P_{S,SS}$	Share of conventional control power at steady-state
$\Delta P_{VSG}(s)$	Change in VSG power
$\Delta P_{VSG,SS}$	Share of VSG power at steady-state

Appendix A

Table A1. Numeric values of control actions used in frequency control loops of the power system.

Control Loop	Proportional Control (P)	Integral Control (I)	Derivative Control (D)
Supplementary	0	−0.05	-
DR	−2.3	−6.1	-
VSG	0.4	0.2	0.1

Appendix B

Figure A1 shows the Simulink model for wind power generation. To simulate the random fluctuations in wind power generation, white noise block of MATLAB/Simulink is used. As shown in Figure A1, the wind speed standard deviation is multiplied by the random output fluctuation provided by the white noise block. The output power, calculated using Equation (A1), is averaged to remove sharp changes.

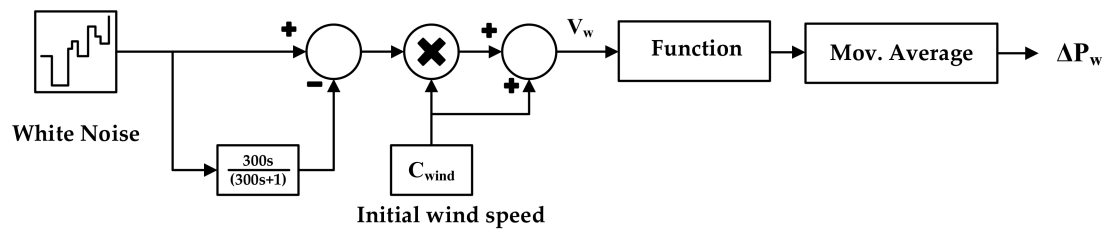


Figure A1. Model for wind power generation.

The wind power is calculated using Equation (B1) as follows. The block “Function” in Figure A1 implements this equation.

$$P_w = 0.5 \times C_p V_w^3 d A \quad (\text{A1})$$

where V_w is wind speed (m/s), C_p is power coefficient, d is air density (kg/m^3), and A is cross-sectional area of wind turbine rotor (m^2). Table A2 shows the values of various parameters used for simulation of wind power generation.

Table A2. Values of various parameters of wind turbine.

Parameter	Value	Unit
V_w , wind speed	7 and 12	m/s
C_p , power coefficient	0.4	
d , is air density	1.293	kg/m^3
A , cross-sectional area of WT rotor	5	m^2

References

- Anderson, P.M.; Fouad, A.A. *Power System Control and Stability*; John Wiley & Sons: Hoboken, NJ, USA, 2008.
- Gelazanskas, L.; Gamage, K.A.A. Demand side management in smart grid: A review and proposals for future direction. *Sustain. Cities Soc.* **2014**, *11*, 22–30. [CrossRef]
- Qdr, Q. Benefits of Demand Response in Electricity Markets and Recommendations for Achieving Them. *US Dept. Energy Wash. DC USA Tech. Rep.* **2006**. Available online: <https://emp.lbl.gov/sites/all/files/report-lbnl-1252d.pdf> (accessed on 2 January 2018).
- Albadi, M.H.; El-Saadany, E.F. A summary of demand response in electricity markets. *Electr. Power Syst. Res.* **2008**, *78*, 1989–1996. [CrossRef]
- Haider, Z.M.; Mehmood, K.K.; Rafique, M.K.; Khan, S.U.; Lee, S.-J.; Kim, C.-H. Water-filling algorithm based approach for management of responsive residential loads. *J. Mod. Power Syst. Clean Energy* **2018**, *6*, 118–131. [CrossRef]
- Tian, J.; Tan, R.; Guan, X.; Liu, T. Enhanced Hidden Moving Target Defense in Smart Grids. *IEEE Trans. Smart Grid* **2018**. [CrossRef]
- Siano, P. Demand response and smart grids—A survey. *Renew. Sustain. Energy Rev.* **2014**, *30*, 461–478. [CrossRef]
- Chen, S.; Liu, T.; Gao, F.; Ji, J.; Xu, Z.; Qian, B.; Wu, H.; Guan, X. Butler, Not Servant: A Human-Centric Smart Home Energy Management System. *IEEE Commun. Mag.* **2017**, *55*, 27–33. [CrossRef]
- Fernández-Blanco, R.; Arroyo, J.M.; Alguacil, N.; Guan, X. Incorporating Price-Responsive Demand in Energy Scheduling Based on Consumer Payment Minimization. *IEEE Trans. Smart Grid* **2016**, *7*, 817–826. [CrossRef]
- Villena, J.; Viguera-Rodríguez, A.; Gómez-Lázaro, E.; Fuentes-Moreno, J.Á.; Muñoz-Benavente, I.; Molina-García, A. An Analysis of Decentralized Demand Response as Frequency Control Support under Critical Wind Power Oscillations. *Energies* **2015**, *8*, 12881–12897. [CrossRef]
- Hajibandeh, N.; Ehsan, M.; Soleymani, S.; Shafie-khah, M.; Catalão, J.P.S. The Mutual Impact of Demand Response Programs and Renewable Energies: A Survey. *Energies* **2017**, *10*, 1353. [CrossRef]
- Shariatzadeh, F.; Mandal, P.; Srivastava, A.K. Demand response for sustainable energy systems: A review, application and implementation strategy. *Renew. Sustain. Energy Rev.* **2015**, *45*, 343–350. [CrossRef]

13. Zehir, M.A.; Batman, A.; Bagriyanik, M. Review and comparison of demand response options for more effective use of renewable energy at consumer level. *Renew. Sustain. Energy Rev.* **2016**, *56*, 631–642. [[CrossRef](#)]
14. Pourmousavi, S.A.; Nehrir, M.H. Real-Time Central Demand Response for Primary Frequency Regulation in Microgrids. *IEEE Trans. Smart Grid* **2012**, *3*, 1988–1996. [[CrossRef](#)]
15. Pourmousavi, S.A.; Nehrir, M.H. Introducing Dynamic Demand Response in the LFC Model. *IEEE Trans. Power Syst.* **2014**, *29*, 1562–1572. [[CrossRef](#)]
16. Kermani, H.R.; Dahraie, M.V.; Najafi, H.R. Demand response strategy for frequency regulation in a microgrid without storage requirement. In Proceedings of the 2016 24th Iranian Conference on Electrical Engineering (ICEE), Shiraz, Iran, 10–12 May 2016; pp. 921–926. [[CrossRef](#)]
17. Short, J.A.; Infield, D.G.; Freris, L.L. Stabilization of Grid Frequency Through Dynamic Demand Control. *IEEE Trans. Power Syst.* **2007**, *22*, 1284–1293. [[CrossRef](#)]
18. Klem, A.; Nehrir, M.H.; Dehghanpour, K. Frequency stabilization of an islanded microgrid using droop control and demand response. In Proceedings of the North American Power Symposium (NAPS), Denver, CO, USA, 18–20 September 2016; pp. 1–6. [[CrossRef](#)]
19. Molina-Garcia, A.; Bouffard, F.; Kirschen, D.S. Decentralized Demand-Side Contribution to Primary Frequency Control. *IEEE Trans. Power Syst.* **2011**, *26*, 411–419. [[CrossRef](#)]
20. Incorporating Demand Response with Spinning Reserve to Realize an Adaptive Frequency Restoration Plan for System Contingencies. *IEEE J. Mag.* **2012**, *3*, 1145–1153. Available online: <http://ieeexplore.ieee.org/document/6213578/> (accessed on 31 January 2018).
21. Bao, Y.-Q.; Li, Y.; Wang, B.; Hu, M.; Zhou, Y. Day-Ahead Scheduling Considering Demand Response as a Frequency Control Resource. *Energies* **2017**, *10*, 82. [[CrossRef](#)]
22. Zakeri, A.S.; Askarian Abyaneh, H. Transmission Expansion Planning Using TLBO Algorithm in the Presence of Demand Response Resources. *Energies* **2017**, *10*, 1376. [[CrossRef](#)]
23. Humayun, M.; Degefa, M.Z.; Safdarian, A.; Lehtonen, M. Utilization Improvement of Transformers Using Demand Response. *IEEE Trans. Power Deliv.* **2015**, *30*, 202–210. [[CrossRef](#)]
24. Elbasuony, G.S.; Abdel Aleem, S.H.E.; Ibrahim, A.M.; Sharaf, A.M. A unified index for power quality evaluation in distributed generation systems. *Energy* **2018**, *149*, 607–622. [[CrossRef](#)]
25. Bukhari, S.B.A.; Saeed Uz Zaman, M.; Haider, R.; Oh, Y.-S.; Kim, C.-H. A protection scheme for microgrid with multiple distributed generations using superimposed reactive energy. *Int. J. Electr. Power Energy Syst.* **2017**, *92*, 156–166. [[CrossRef](#)]
26. Bhadane, K.V.; Ballal, M.S.; Moharil, R.M. Investigation for Causes of Poor Power Quality in Grid Connected Wind Energy—A Review. In Proceedings of the 2012 Asia-Pacific Power and Energy Engineering Conference, Shanghai, China, 27–29 March 2012; pp. 1–6.
27. Ali, M.A.S.; Mehmood, K.K.; Kim, C.-H. Power System Stability Improvement through the Coordination of TCPS-based Damping Controller and Power System Stabilizer. *Adv. Electr. Comput. Eng.* **2017**, *17*, 27–36. [[CrossRef](#)]
28. Krismanto, A.U.; Mithulananthan, N.; Krause, O. Stability of Renewable Energy based Microgrid in Autonomous Operation. *Sustain. Energy Grids Netw.* **2018**, *13*, 134–147. [[CrossRef](#)]
29. Bevrani, H. *Robust Power System Frequency Control*; Power Electronics and Power Systems; Springer International Publishing: Cham, Switzerland, 2014; ISBN 978-3-319-07277-7.
30. Zhong, Q.-C.; Weiss, G. Synchronverters: Inverters That Mimic Synchronous Generators. *IEEE Trans. Ind. Electron.* **2011**, *58*, 1259–1267. [[CrossRef](#)]
31. Balijepalli, V.S.K.M.; Ukil, A.; Karthikeyan, N.; Gupta, A.K.; Shicong, Y. Virtual synchronous generators as potential solution for electricity Grid compliance studies. In Proceedings of the 2016 IEEE Region 10 Conference (TENCON), Singapore, 22–25 November 2016; pp. 718–722.
32. Tamrakar, U.; Shrestha, D.; Maharjan, M.; Bhattarai, B.P.; Hansen, T.M.; Tonkoski, R. Virtual Inertia: Current Trends and Future Directions. *Appl. Sci.* **2017**, *7*, 654. [[CrossRef](#)]
33. Hirase, Y.; Abe, K.; Sugimoto, K.; Sakimoto, K.; Bevrani, H.; Ise, T. A novel control approach for virtual synchronous generators to suppress frequency and voltage fluctuations in microgrids. *Appl. Energy* **2018**, *210*, 699–710. [[CrossRef](#)]
34. Li, C.; Xu, J.; Zhao, C. A Coherency-Based Equivalence Method for MMC Inverters Using Virtual Synchronous Generator Control. *IEEE Trans. Power Deliv.* **2016**, *31*, 1369–1378. [[CrossRef](#)]

35. Ma, Y.; Cao, W.; Yang, L.; Wang, F.; Tolbert, L.M. Virtual Synchronous Generator Control of Full Converter Wind Turbines with Short-Term Energy Storage. *IEEE Trans. Ind. Electron.* **2017**, *64*, 8821–8831. [[CrossRef](#)]
36. Liu, J.; Miura, Y.; Bevrani, H.; Ise, T. Enhanced Virtual Synchronous Generator Control for Parallel Inverters in Microgrids. *IEEE Trans. Smart Grid* **2017**, *8*, 2268–2277. [[CrossRef](#)]
37. Kerdphol, T.; Rahman, F.; Mitani, Y.; Hongesombut, K.; Küfeoğlu, S. Virtual Inertia Control-Based Model Predictive Control for Microgrid Frequency Stabilization Considering High Renewable Energy Integration. *Sustainability* **2017**, *9*, 773. [[CrossRef](#)]
38. Qi, Y.; Wang, D.; Wang, X.; Jia, H.; Pu, T.; Chen, N.; Liu, K. Frequency Control Ancillary Service Provided by Efficient Power Plants Integrated in Queuing-Controlled Domestic Water Heaters. *Energies* **2017**, *10*, 559. [[CrossRef](#)]
39. Nisar, A.; Thomas, M.S. Comprehensive Control for Microgrid Autonomous Operation with Demand Response. *IEEE Trans. Smart Grid* **2017**, *8*, 2081–2089. [[CrossRef](#)]
40. Chen, Y.; Hesse, R.; Turschner, D.; Beck, H.P. Improving the grid power quality using virtual synchronous machines. In Proceedings of the 2011 International Conference on Power Engineering, Energy and Electrical Drives, Malaga, Spain, 11–13 May 2011; pp. 1–6.
41. Kerdphol, T.; Qudaih, Y.; Mitani, Y. Optimum battery energy storage system using PSO considering dynamic demand response for microgrids. *Int. J. Electr. Power Energy Syst.* **2016**, *83*, 58–66. [[CrossRef](#)]
42. Tan, Z.; Li, H.; Ju, L.; Song, Y. An Optimization Model for Large-Scale Wind Power Grid Connection Considering Demand Response and Energy Storage Systems. *Energies* **2014**, *7*, 7282–7304. [[CrossRef](#)]
43. Dorf, R.C.; Bishop, R.H. *Modern Control Systems*, 12th ed.; Pearson: Prentice Hall: New York, NY, USA, 2010; ISBN 978-0-13-602458-3.
44. Albu, M.; Nechifor, A.; Creanga, D. Smart storage for active distribution networks estimation and measurement solutions. In Proceedings of the 2010 IEEE Instrumentation & Measurement Technology Conference, Austin, TX, USA, 3–6 May 2010; pp. 1486–1491.
45. Karapanos, V.; de Haan, S.; Zwetsloot, K. Testing a virtual synchronous generator in a real time simulated power system. In Proceedings of the International Conference on Power Systems Transients (IPST), Delft, The Netherlands, 14 June–17 July 2011.
46. Sondhi, S.; Hote, Y.V. Fractional order PID controller for load frequency control. *Energy Convers. Manag.* **2014**, *85*, 343–353. [[CrossRef](#)]
47. IEEE Recommended Practice for Functional and Performance Characteristics of Control Systems for Steam Turbine-Generator Units. IEEE Std. 122-1991. 1992. Available online: <http://ieeexplore.ieee.org/iel1/2432/1139/00027883.pdf> (accessed on 12 December 2017). [[CrossRef](#)]



© 2018 by the authors. Licensee MDPI, Basel, Switzerland. This article is an open access article distributed under the terms and conditions of the Creative Commons Attribution (CC BY) license (<http://creativecommons.org/licenses/by/4.0/>).